

Interference through the resonant Auger process via multiple core-excited states

Souvik Chatterjee*

*Department of Chemistry, Sikkim University, Gangtok, Sikkim 737102, India
and Institute of Advanced Energy, Kyoto University, Gokasho, Uji, Kyoto 611-0011, Japan*

Takashi Nakajima†

Institute of Advanced Energy, Kyoto University, Gokasho, Uji, Kyoto 611-0011, Japan

(Received 6 June 2017; published 6 December 2017)

We theoretically investigate the resonant Auger process via multiple core-excited states. The presence of multiple core-excited states sets off interference into the common final continuum, and we show that the degree of interference depends on the various parameters such as the intensity of the employed x-ray pulse and the lifetimes of the core-excited states. For the specific examples we employ the double ($1s^{-1}3p$ and $1s^{-1}4p$) core-excited states of Ne atom and numerically solve the time-dependent Schrödinger equation to demonstrate that the energy-resolved electron spectra clearly exhibit the signature of interference.

DOI: [10.1103/PhysRevA.96.063406](https://doi.org/10.1103/PhysRevA.96.063406)

I. INTRODUCTION

The recent availability of x-ray free electron lasers (FELs) has opened up the opportunities to scrutinize some of the inner-shell processes, which have been studied earlier using synchrotron radiation, for deeper understanding of the inner-shell electron dynamics. The decay of a resonantly produced core-excited state into the continuum, called the resonant Auger (RA) process, is one of the inner-shell processes [1] that have been under the intensive study using the recently developed x-ray laser sources [2–7]. If a weak laser pulse or synchrotron radiation is employed to induce the resonant core-excitation, the RA process dominates far over the direct photoionization processes from the ground state. This means that the interference does not occur during the RA process under such conditions. However, the latter process can be of a magnitude comparable to that of the former one if the laser pulse becomes intense, and, accordingly, interference can occur. Obviously, the RA processes induced by the intense x-ray pulse have a new aspect and can lead to the new realm of rich physics.

As mentioned above, the RA and direct photoionization processes starting from the ground state into the common final (continuum) state can interfere, and the degree of interference becomes stronger as the x-ray laser pulse becomes more intense [2,3,8–13]. The intense x-ray pulse for the resonant excitation of core-excited state also induces the Rabi oscillation between the ground and core-excited states. This Rabi oscillation manifests itself as the line splitting in the RA electron spectrum, and this is another interesting phenomenon in the high-intensity regime [2–7]. Similar line splitting was observed previously in the autoionization [14], resonant fluorescence [15], and resonant multiphoton ionization [16,17] processes, respectively.

Beyond the simplest use of the single-color x-ray pulse, the RA processes are also studied using a two-color (x-ray + optical or x-ray + x-ray) laser field to deeply probe the inner-shell processes [18–31]. Recently, theoretical studies

using the ultrashort x-ray pulses have been extended for the RA processes involving more than single core-excited states [30,31]. Such a study is realistic, because the ultrashort x-ray pulse, which necessarily has a broad bandwidth, can excite more than one core-excited state. In this paper we theoretically investigate the RA processes via multiple (two) core-excited states and demonstrate that the RA process under such situations can exhibit an interference pattern in the energy-resolved electron spectra.

II. THEORY

We employ the time-dependent Schrödinger equation to describe all the different processes which are triggered upon exposure of the Ne atom to a strong ultrashort x-ray laser pulse. Figure 1 shows the relevant levels. We consider the ground state $|g\rangle$ ($1s^2 2s^2 2p^6$ at 0 eV) and two core-excited states, $|a_1\rangle$ ($1s^{-1}3p$ at 867.1 eV) and $|a_2\rangle$ ($1s^{-1}4p$ at 868.7 eV). Upon exposure to the resonant x-ray pulse, the RA process as well as direct photoionization process from the ground state (Process A) take place. Additionally, photoionization from the two core-excited states (Process B) also occurs. All these processes are depicted in Fig. 1. More precisely, after the promotion of inner electrons to the two core-excited states, $|a_1\rangle$ and $|a_2\rangle$, the produced core-excited states decay through the RA process into the two continua, $|f_{1,\varepsilon_1}\rangle$ ($\text{Ne}^+ 2p^4 3p$ at 55.8 eV + free electron) and $|f_{2,\varepsilon_1}\rangle$ ($\text{Ne}^+ 2p^4 4p$ at 59.8 eV + free electron), where ε_k ($k = 1, 2$) denotes the energy of the free electron ejected into the continuum and f_k ($k = 1, 2$) denotes the final ionic states, Ne^+ , formed after the RA decay from states $|a_1\rangle$ and $|a_2\rangle$, respectively. Although both core-excited states can decay into both continua, the dominant channels are $|a_1\rangle \rightarrow |f_{1,\varepsilon_1}\rangle$ and $|a_2\rangle \rightarrow |f_{2,\varepsilon_2}\rangle$.

The total time-dependent wave function of the system, $\Psi(t)$, shown in Fig. 1 can be expanded as [2,3,6,30]

$$\begin{aligned} \Psi(t) = & c_g(t)|g\rangle + e^{-i\omega t}[c_{a_1}(t)|a_1\rangle + c_{a_2}(t)|a_2\rangle] \\ & + \int e^{-i\omega t} c_{f_1}(\varepsilon_1, t) |f_{1,\varepsilon_1}\rangle d\varepsilon_1 \\ & + \int e^{-i\omega t} c_{f_2}(\varepsilon_2, t) |f_{2,\varepsilon_2}\rangle d\varepsilon_2, \end{aligned} \quad (1)$$

*svkch08@gmail.com

†nakajima@iae.kyoto-u.ac.jp

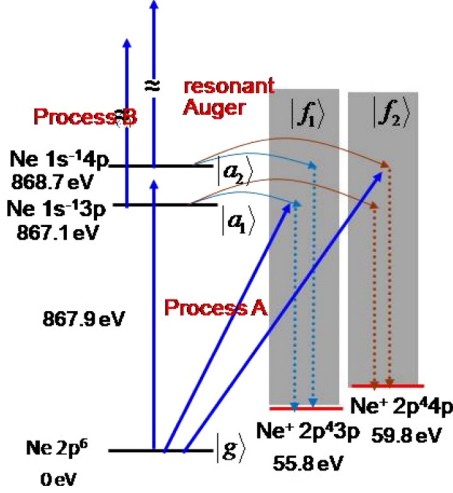


FIG. 1. Level scheme of the theoretical model. Upon exposure of the Ne atom to a resonant x-ray laser pulse the RA process via two core-excited states, $|a_1\rangle$ ($1s^{-1}3p$) and $|a_2\rangle$ ($1s^{-1}4p$), as well as direct photoionization process (Process A) from the ground state, $|g\rangle$ ($2p^6$), take place, and both processes bring atoms into the common continuum states, $|f_1, \epsilon_1\rangle$ (Ne $^+$ $2p^4 3p$ + free electron) and $|f_2, \epsilon_2\rangle$ (Ne $^+$ $2p^4 4p$ + free electron). Although Process A is usually very weak and may be even negligible, it can become as strong as that of the RA process when the incident x-ray pulse is very strong, which is our case. The interference between the two processes can be seen, for example, in the energy-resolved electron spectra, as we will show in this paper. For completeness, we also include the photoionization process from the core-excited states (Process B). Note that Process B is not negligible either when the incident x-ray pulse is strong, and it can affect the probability amplitudes of the core-excited states, resulting in the RA process also being influenced.

where ω is the central frequency of the x-ray pulse, and $c_m(t)$ ($m = g, a_1, a_2$) and $c_{f_k}(t)$ ($k = 1, 2$) denote the time-dependent probability amplitudes of the states indicated by the subscripts. After invoking the rotating-wave approximation, we obtain the following set of coupled differential equations. It reads

$$\begin{aligned}
 i\dot{c}_g(t) &= \left[E_g - \frac{i}{2}\gamma_g(t) \right] c_g(t) \\
 &+ \sum_{i=1,2} \left[D_{a_i g}^\dagger - i\pi \sum_{j=1,2} D_{f_j g}^\dagger(t) V_{f_j a_i} \right] c_{a_i}(t), \quad (2) \\
 i\dot{c}_{a_1}(t) &= \left[E_{a_1} - \omega - \frac{i}{2}[\Gamma_{a_1} + \gamma_{a_1}(t)] \right] c_{a_1}(t) \\
 &+ \left[D_{a_1 g} - i\pi \sum_{j=1,2} V_{f_j a_1}^\dagger D_{f_j g}(t) \right] c_g(t) \\
 &- i\pi \left[\sum_{j=1,2} V_{f_j a_1}^\dagger V_{f_j a_2} \right] c_{a_2}(t), \quad (3) \\
 i\dot{c}_{a_2}(t) &= \left[E_{a_2} - \omega - \frac{i}{2}[\Gamma_{a_2} + \gamma_{a_2}(t)] \right] c_{a_2}(t)
 \end{aligned}$$

$$\begin{aligned}
 &+ \left[D_{a_2 g} - i\pi \sum_{j=1,2} V_{f_j a_2}^\dagger D_{f_j g}(t) \right] c_g(t) \\
 &- i\pi \left[\sum_{j=1,2} V_{f_j a_1} V_{f_j a_2}^\dagger \right] c_{a_1}(t), \quad (4) \\
 i\dot{c}_{f_j}(\epsilon_j, t) &= [E_{f_j} + \epsilon_j - \omega] c_{f_j}(\epsilon_j, t) \\
 &+ D_{f_j g}(t) c_g(t) + V_{f_j a_1} c_{a_1}(t) \\
 &+ V_{f_j a_2} c_{a_2}(t) \quad (j = 1, 2). \quad (5)
 \end{aligned}$$

In the above equations E_m are the energies of neutral atomic states, $|m\rangle$ ($m = g, a_1, a_2$), while E_{f_j} ($j = 1, 2$) are the energies of the final continuum states which are formed after the RA decay or direct photoionization from the ground state. The total Auger decay rate from state $|k\rangle$ ($k = a_1, a_2$) is expressed as Γ_k . $V_{f_j a_i}$ are the Coulomb matrix elements between the core-excited states, $|a_i\rangle$ ($i = 1, 2$), and the associated continuum states, $|f_j, \epsilon_j\rangle$ ($j = 1, 2$), through the RA decay. They are related to the partial Auger decay rates, $\Gamma_{f_j}^{(a_i)}$ [32,33], through the relation of

$$\Gamma_{f_j}^{(a_i)}(\epsilon_j) = 2\pi |V_{f_j a_i}(\epsilon_j)|^2. \quad (6)$$

We assume that $V_{f_j a_i}$ is constant over the continuum energies of interest, ϵ_j , because of the slow variation of the Coulomb matrix elements, $V_{f_j a_i}$, with energy, ϵ_k ($k = 1, 2$). This is a reasonable assumption for the Auger process with high kinetic energy [1]. The term $\gamma_g(t)$ is the direct photoionization width from the ground state by the x-ray pulse, while $\gamma_k(t)$ are the photoionization width from the core-excited states, $|k\rangle$ ($k = a_1, a_2$), respectively. $D_{a_i g}$ ($i = 1, 2$) are the Rabi frequencies between states $|g\rangle$ and $|a_i\rangle$, and they are expressed as

$$D_{a_i g} = \frac{1}{2} \mu_{a_i g} E(t), \quad (7)$$

in which $\mu_{a_i g}$ ($i = 1, 2$) are the dipole matrix elements between states $|g\rangle$ and $|a_i\rangle$ ($i = 1, 2$). The field amplitude of the x-ray pulse, $E(t)$, is assumed to have a Gaussian temporal profile, and it is expressed as

$$E(t) = E_0 \exp \left[-4 \ln 2 \left(\frac{t}{\sigma} \right)^2 \right], \quad (8)$$

where σ is the duration of x-ray pulse defined for the full width at half maximum (FWHM) for the field envelope, with E_0 being the peak field amplitude. The bound-free matrix element from the ground state, $|g\rangle$, to the continuum, $|f_j, \epsilon_j\rangle$ ($j = 1, 2$), associated with Process A in Fig. 1 is expressed as

$$D_{f_j g}(\epsilon_j, t) = \frac{1}{2} \mu_{f_j g}(\epsilon_j) E_x(t), \quad (9)$$

where $\mu_{f_j g}$ is the dipole moment between the ground state, $|g\rangle$, and the continuum states, $|f_j, \epsilon_j\rangle$ ($j = 1, 2$).

We study the RA process induced by the intense x-ray pulse by calculating the energy-resolved electron spectra after a sufficiently long time to ensure the complete decay of the core-excited states into the continuum.

The energy-resolved electron spectra, $P(\epsilon_j)$, into the two continua, $|f_j, \epsilon_j\rangle$ ($j = 1, 2$), through the RA process is

computed using the relation of

$$P(\varepsilon_j) = \lim_{t \rightarrow \infty} |c_{f_j}(\varepsilon_j, t)|^2. \quad (10)$$

III. NUMERICAL RESULTS AND DISCUSSIONS

The photon energy and the duration of the x-ray pulses used to compute the electron spectra are 867.9 eV and 2.4 fs (which is comparable to the lifetime of the core-excited states of Ne, $1s^{-1}3p$ and $1s^{-1}4p$), respectively, unless otherwise mentioned. This photon energy falls midway between the two core-excited states; i.e., $E_{a_1} - \omega = E_{a_2} - \omega$. The relevant dipole matrix elements are $\mu_{a_1g} = 0.0096$ (au) [21] and $\mu_{a_2g} = 0.0059$ (au), respectively [10], and the lifetimes of the core-excited states are 2.41 fs for both $|a_1\rangle$ and $|a_2\rangle$. The partial Auger decay rates of the two core-excited states decaying into the two continuum states, $|f_1, \varepsilon_1\rangle$ and $|f_2, \varepsilon_1\rangle$, are assumed to be constant over the continuum energies, as mentioned before. The ionization width of the ground state, γ_g , and the transition matrix element, μ_{f_1g} , are calculated from the direct and partial photoionization cross sections of 2.4×10^{-20} cm² and 0.06×10^{-20} cm², respectively [2]. We assume that $\mu_{f_2g} = \mu_{f_1g}$. The ionization widths, γ_{a_1} and γ_{a_2} , from the core-excited states, a_1 and a_2 , respectively, are also assumed to be equal, and they are calculated from the value of the photoionization cross section, 3.2×10^{-20} cm², reported in Ref. [21]. The Coulomb matrix elements (a.u.) used for the calculations are $V_{f_1a_1} = 3.4 \times 10^{-2}$, $V_{f_2a_1} = 2.1 \times 10^{-2}$, $V_{f_1a_2} = 0.69 \times 10^{-2}$, and $V_{f_2a_2} = 1.8 \times 10^{-2}$, respectively. These Coulomb matrix elements are calculated from the relative partial decay width, defined as $\Gamma_{f_j}^{(a_i)} / \Gamma_k$ in Ref. [10].

It has been found in recent studies that the energy-resolved electron spectra obtained by the intense resonant x-ray pulse exhibit an asymmetric line splitting [2,3,6,7], which is interpreted to appear as a result of the interplay between the rapid Rabi oscillations, RA process, and direct photoionization process [34]. More precisely, the origin of such multiple peak structures has been interpreted as dynamic interference between electron wave packets with the same kinetic energy but ejected at different times during the x-ray pulse [34]. However, in their work the energy-resolved electron spectra have been calculated for the case of single core-excited state.

In this work we calculate the energy-resolved electron spectra for the case of a superposition of two core-excited states, $|a_1\rangle$ and $|a_2\rangle$, decaying into the common continuum, f_1 . We calculate the energy-resolved electron spectra by including all possible ionization processes (= RA process + Process A + Process B) [Fig. 2(a)], RA process and Process A [Fig. 2(b)], and RA process only [Fig. 2(c)], respectively. We first look into the results which include both RA decay channels [black solid lines in Figs. 2(a)–2(c)]. For all three cases [Figs. 2(a)–2(c)] the line shapes turn out to be asymmetric with multiple peak structures. However, the peak positions and the line shape are all different, depending on the ionization processes included for the calculations: In Figs. 2(a) and 2(b) the asymmetric line splitting with a central peak at around 812 eV and a side peak at 811.2 eV is observed. This side peak is very subtle in Fig. 2(c). The asymmetric line splitting in Figs. 2(a)–2(c) is attributed to the Rabi oscillations between the ground and core-excited states [2–4,6,7,34]. The barely visible peak around 811.2 eV

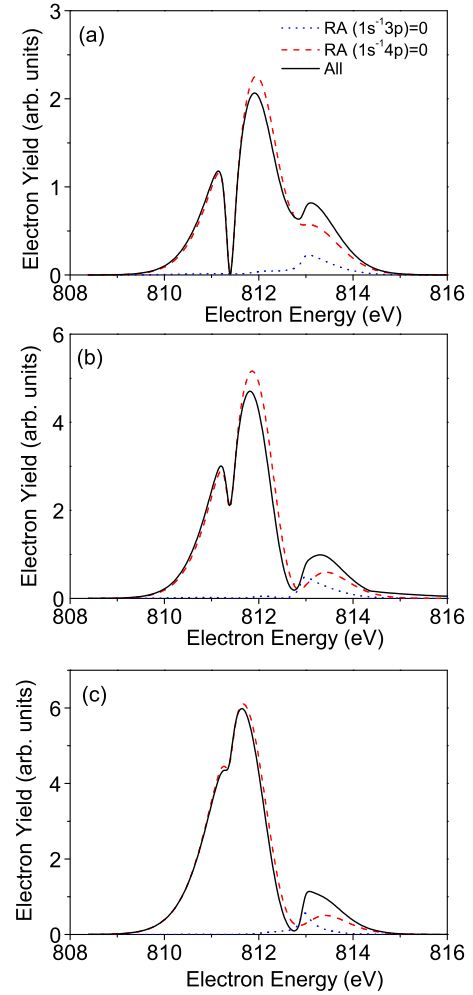


FIG. 2. Energy-resolved electron spectra associated with the f_1 continuum calculated by including (a) all processes (i.e., RA process and Processes A and B), (b) RA process and Process A, and (c) RA process only for the x-ray pulse with the peak intensity of $I_0 = 5 \times 10^{18}$ W/cm². In graphs (a)–(c) the results obtained by including the RA decay channels via $|a_2\rangle$ only, via $|a_1\rangle$ only, and via both $|a_1\rangle$ and $|a_2\rangle$ are plotted by the blue dotted, red dashed, and black solid lines, respectively.

in Fig. 2(c) is more significant in Figs. 2(a) and 2(b) when the direct ionization process (Process A) is included. This is primarily due to the interference between the two pathways, ground state \rightarrow core-excited state $\rightarrow f_1$ continuum and ground state $\rightarrow f_1$ continuum. Note that the signature of such interference has been reported in Refs. [2,3] for the system involving a *single* core-excited state.

To highlight what is special about our system involving the *two* core-excited states instead of the single core-excited state, we perform further calculations by hypothetically turning off the RA decay channels via $|a_2\rangle$ or $|a_1\rangle$. The results are shown by the red dashed and blue dotted lines, respectively, in Figs. 2(a)–2(c). By comparing Fig. 2(b) with Fig. 2(a), we notice that the absence of photoionization from the core-excited state (Process B) leads to the modification in the shape of the electron spectrum, and the central peak at around 812 eV is considerably higher in Fig. 2(b). This is because

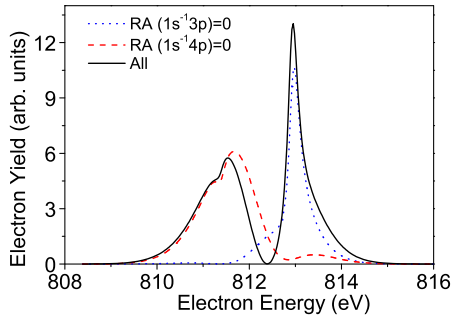


FIG. 3. Similar to Fig. 2(c) with all parameters, except for $\Gamma_{f_1}^{(a_2)}$, chosen to be the same. $\Gamma_{f_1}^{(a_2)}$ is now hypothetically set to be the same with $\Gamma_{f_1}^{(a_1)}$ so that the influence of the RA decay channel via $|a_2\rangle$ becomes comparable with that via $|a_1\rangle$ to better understand the role of the two core-excited states.

the photoionization processes from the core-excited states are turned off for Fig. 2(b), and accordingly the RA processes from those states do not suffer from the population loss. Moreover, the peak at around 813.5 eV is broader in Fig. 2(b).

Now, the important question is whether the shape of the energy-resolved electron spectra shown in Figs. 2(a)–2(c) is determined solely by the two effects, namely the Rabi oscillations between the ground and core-excited states, which results in the ac Stark splitting, and the interference between the two pathways, ground state \rightarrow core-excited state \rightarrow f_1 continuum and ground state \rightarrow f_1 continuum. By comparing the black solid and red dashed lines in each of Figs. 2(a) and 2(b), we find that the contribution of the RA decay process via $|a_1\rangle$ to the electron energy spectrum is far dominant over the one via $|a_2\rangle$. This is because the contribution of the RA decay process via $|a_2\rangle \rightarrow |f_1, \varepsilon_1\rangle$ is much weaker than that via $|a_1\rangle \rightarrow |f_1, \varepsilon_1\rangle$, and accordingly the electron energy spectrum is dominated by the contribution from the RA process via the latter as well as Processes A and B. We find that, even under the very special condition of no RA decay channel, i.e., $|a_1\rangle \leftrightarrow |f_1, \varepsilon_1\rangle$ (i.e., $\Gamma_{f_1}^{(a_1)} = 0$) or $|a_2\rangle \leftrightarrow |f_1, \varepsilon_1\rangle$ (i.e., $\Gamma_{f_1}^{(a_2)} = 0$), the energy-resolved electron spectra clearly show the line splittings [blue dotted and red dashed lines Figs. 2(a)–2(c)], as well as the signature of possible interferences between the RA process and Process A [Figs. 2(a) and 2(b)]. We can say that the shape of the energy-resolved electron spectra labeled as “All” [black solid lines in Figs. 2(a)–2(c)] is mainly determined by the two factors, i.e., the Rabi oscillations between the ground and two core-excited states and the interference between the RA process and Process A.

Now, while we still focus on the energy-resolved electron spectra associated with the f_1 continuum, we hypothetically assume that the RA decay rates from the two core-excited states, $\Gamma_{f_1}^{(a_1)}$ and $\Gamma_{f_1}^{(a_2)}$, are of comparable magnitude so that we can emphasize the importance of the two core-excited states considered in this work. For this we assume both Coulomb matrix elements, $V_{f_1 a_1}$ and $V_{f_1 a_2}$, are equal to 3×10^{-2} . For clarity, we include only the RA process and neglect the photoionization processes, Processes A and B. The results are shown in Fig. 3. The energy-resolved electron spectra obtained by turning off the RA decay channel via $|a_2\rangle$ by setting $\Gamma_{f_1}^{(a_2)} = 0$

(red dashed line in Fig. 3) and via $|a_1\rangle$ by setting $\Gamma_{f_1}^{(a_1)} = 0$ (blue dotted line in Fig. 3) are significantly different, in terms of the height and the position of the peaks, from the original one, which includes the RA decay channel via both (black solid line in Fig. 3). This can be interpreted to arise from interference between the Auger electron released into the f_1 continuum from the two core-excited states, $|a_1\rangle$ and $|a_2\rangle$, respectively. Although the peaks associated with the RA process via $|a_1\rangle$ and $|a_2\rangle$ are usually well separated in the electron energy, interference in the common continuum becomes possible in our system because of the Rabi splittings between the ground and the two core-excited states due to the use of high-intensity x-ray pulse. This results in the substantial overlap between the ejected electrons, which significantly modifies the electron spectrum. Obviously, this kind of interference is absent when only a single core-excited state is involved in the system. Note, however, that the study of the electron spectra associated with the f_1 continuum is not the most convenient method by which to clarify the difference between the systems involving the two core-excited states and the single core-excited state, because the partial RA rate via $|a_1\rangle$ into the f_1 continuum is far larger than that via $|a_2\rangle$. That is why the red dashed lines almost completely overlap with the solid black lines in Fig. 2.

In the case of the f_2 continuum, the Coulomb matrix elements, $V_{f_2 a_2}$ and $V_{f_2 a_1}$, are comparable in magnitude and hence provide us with a realistic situation of the hypothetical case studied in Fig. 3. Similar to Fig. 2, showing the energy-resolved electron spectra associated with the f_1 continuum, we calculate the energy-resolved electron spectra associated with the f_2 continuum under the three different conditions, and the results are shown in Figs. 4(a)–4(c). By turning off the RA decay via one of the two core-excited states, a significant modification in the peak position and amplitude for all the three cases are evident in Figs. 4(a)–4(c). That is, unlike Fig. 2, none of the three lines with solid black, red dashed, and blue dotted lines overlap in Fig. 4. The central peak of the original spectrum at around 807.5 eV in Fig. 4(c) shows a bifurcation, which is absent if $\Gamma_{f_2}^{(a_2)} = 0$ (red dashed line). All these features we find in Fig. 4 are reminiscent of the energy-resolved electron spectra shown in Fig. 3, which have been calculated under the hypothetical assumption that $\Gamma_{f_1}^{(a_1)} = \Gamma_{f_1}^{(a_2)}$. The origin of the unresolved line splitting at around 807.2 eV when all processes are involved [solid line in Fig. 4(c)] can be attributed to the interference between the electrons released via the two core-excited states into the f_2 continuum. The results in Figs. 3 and 4(c) are similar, because in both cases the partial Auger decay rate from the two core-excited states are of comparable magnitude and hence the degree of interference between the emitted electrons from the two core-excited states will be similar. The only difference is that the interference between the emitted electrons from two different core-excited states is taking place in two different continua f_1 (f_2) for Fig. 3 (Fig. 4).

From the above results and discussions we can claim that the system involving the two core-excited states exhibits another kind of interference through the RA decay via two core-excited states, which is obviously absent if only one core-excited state is involved. To prove that this is a high-intensity effect, we calculate the energy-resolved electron spectra associated with the f_2 continuum at the modest peak intensity of

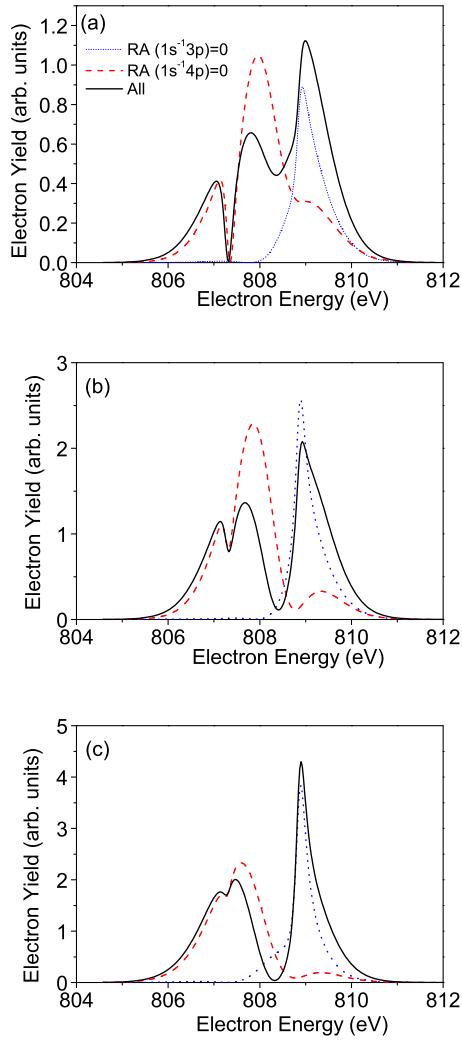


FIG. 4. Similar to Fig. 2, but the energy-resolved electron spectra are associated with the f_2 continuum.

$I^0 = 10^{16}$ W/cm², and the results are shown in Fig. 5. Here also for clarity we have considered the RA process only. At this intensity the additional contribution to the linewidth of the core-excited states due to the power broadening is negligibly small, and hence the interference in the common continuum through the RA decay via the two core-excited states can occur

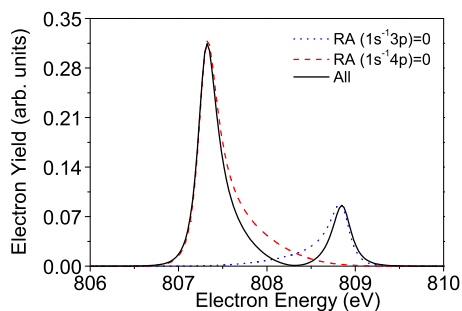


FIG. 5. Energy-resolved electron spectra associated with the f_2 continuum for the modest peak intensity of the x-ray pulse at $I_0 = 10^{16}$ W/cm².

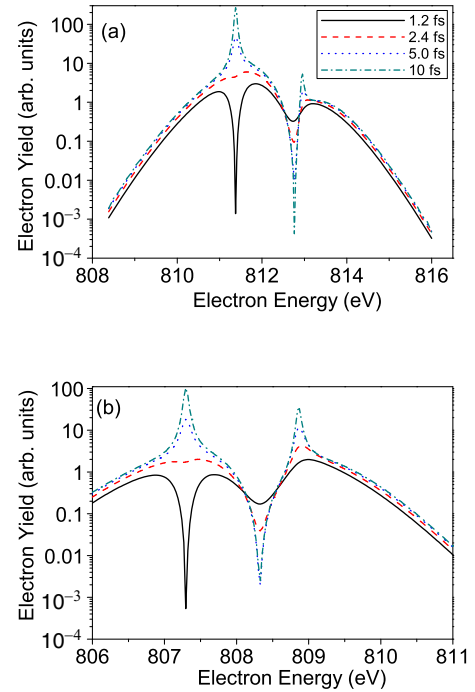


FIG. 6. Energy-resolved electron spectra associated with the (a) f_1 and (b) f_2 continua calculated assuming hypothetical lifetimes of 1.2 fs (solid lines), 2.4 fs (dashed lines), 5 fs (dotted lines), and 10 fs (dashed dotted lines), respectively. The x-ray pulse intensity is same as that of Fig. 2. The results are plotted in log scale.

only at the valley between the two resonance energies, as we notice in Fig. 5.

As a final proof of our claim we calculate the energy-resolved electron spectrum, for the RA process only, associated with the f_1 and f_2 continua with the hypothetically modified lifetimes (RA decay rates) of core-excited states. The results are shown in Figs. 6(a) and 6(b), respectively. A shorter (longer) lifetime means that the natural linewidth of the core-excited state is broader (narrower) due to the faster (slower) RA decay rate. As a result, for the system with the hypothetically shorter lifetimes, the interference through the RA decay process via the two core-excited states into the common final continuum can occur at the resonance which turns up as a deep valley [solid black lines in Figs. 6(a) and 6(b)]. If the lifetimes are longer, only the two sharper resonant peaks appear, as usual, without any signature of interference [red dashed \rightarrow blue dotted \rightarrow green dot-dashed lines in Figs. 6(a) and 6(b)].

IV. CONCLUSIONS

We have theoretically investigated the resonant Auger processes of Ne atoms exposed to an intense x-ray pulse with a duration of a few femtoseconds. Unlike most of the other related studies, multiple core-excited states are involved in our study, which could supposedly induce interference through the resonant Auger decay. For the minimum number of multiplicity, i.e., two core-excited states, we have shown that this is indeed the case, and only if the intensity of the x-ray

pulse is sufficiently high or the lifetimes of the core-excited states are sufficiently short, the energy-resolved electron spectra exhibit the additional structure which originates from interference through the resonant Auger process via the two core-excited states. We have also clarified that the interference occurs only in the electron energy region with a sufficient overlap between the core-excited states. To go beyond the two core-excited states is straightforward, but would not bring a new phenomenon, because, as we have seen in this

work, the RA rate rapidly decreases as the state energy increases.

ACKNOWLEDGMENTS

This work was supported by the Grant-in-Aid for scientific research from the Ministry of Education, Culture, Sports, Science and Technology of Japan. The work by S.C. was also supported by the Research Grant from the Department of Science and Technology, India under Inspire program.

-
- [1] G. B. Armen, H. Aksela, T. Åberg, and S. Aksela, The resonant Auger effect, *J. Phys. B* **33**, R49 (2000).
- [2] Ph. V. Demekhin and L. S. Cederbaum, Strong interference effects in the resonant Auger decay of atoms induced by intense x-ray fields, *Phys. Rev. A* **83**, 023422 (2011).
- [3] S. Chatterjee and T. Nakajima, Manipulation of resonant Auger processes using a strong bichromatic field, *Phys. Rev. A* **91**, 043413 (2015).
- [4] J.-C. Liu, Y.-P. Sun, C.-K. Wang, H. Ågren, and F. Gel'mukhanov, Auger effect in the presence of strong x-ray pulses, *Phys. Rev. A* **81**, 043412 (2010).
- [5] Y.-P. Sun, J.-C. Liu, C.-K. Wang, and F. Gel'mukhanov, Propagation of a strong x-ray pulse: Pulse compression, stimulated Raman scattering, amplified spontaneous emission, lasing without inversion, and four-wave mixing, *Phys. Rev. A* **81**, 013812 (2010).
- [6] N. Rohringer and R. Santra, Resonant Auger effect at high x-ray intensity, *Phys. Rev. A* **77**, 053404 (2008).
- [7] E. P. Kanter *et al.*, Unveiling and Driving Hidden Resonances with High-Fluence, High-Intensity X-ray Pulses, *Phys. Rev. Lett.* **107**, 233001 (2011).
- [8] R. Camilloni, M. Žitnik, C. Comicioli, K. C. Prince, M. Zaccagna, C. Crotti, C. Ottaviani, C. Quaresima, P. Perfetti, and G. Stefani, Interference Effects in the Auger Decay of the Resonantly Excited $2p^{-1} \frac{3}{2} 3d$ State of Argon, *Phys. Rev. Lett.* **77**, 2646 (1996).
- [9] E. Kukk, H. Aksela, A. Kivimäki, J. Jauhiainen, E. Nömmiste, and S. Aksela, Electronic-state lifetime interference in the resonant Auger decay of krypton, *Phys. Rev. A* **56**, 1481 (1997).
- [10] N. Saito, N. M. Kabachnik, Y. Shimizu, H. Yoshida, H. Ohashi, Y. Tamenori, I. H. Suzuki, and K. Ueda, Interference effects in the branching ratio for the partial decay channels of the Ne($1s^{-1}3p$) resonance, *J. Phys. B* **33**, L729 (2000).
- [11] B. M. Lagutin, Ph. V. Demekhin, V. L. Sukhorukov, A. Ehresmann, and H. Schmoranzer, Interference effects in Auger spectra at the $3d^{-9}np$ resonances in Kr, *J. Phys. B* **36**, L163 (2003).
- [12] B. M. Lagutin, I. D. Petrov, V. L. Sukhorukov, S. Kammer, S. Mickat, R. Schill, K.-H. Schartner, A. Ehresmann, Yu. A. Shutov, and H. Schmoranzer, Raman Regime Energy Dependence of Alignment and Orientation of KrI States Populated by Resonant Auger Effect, *Phys. Rev. Lett.* **90**, 073001 (2003).
- [13] B. M. Lagutin, I. D. Petrov, V. L. Sukhorukov, Ph. V. Demekhin, B. Zimmermann, S. Mickat, S. Kammer, K.-H. Schartner, A. Ehresmann, Yu. A. Shutov, and H. Schmoranzer, The interference effects in the alignment and orientation of the Kr II $4p^{-4}5p$ states following Kr I $3d^{-9}np$ resonance excitation, *J. Phys. B* **36**, 3251 (2003).
- [14] K. Rzażewski, Strong-field autoionization by $2\pi n$ pulses and multiplex photoelectron spectrum, *Phys. Rev. A* **28**, 2565 (1983).
- [15] E. J. Robinson, Temporal 'diffraction' and eigenvalue interpretation of the resonance fluorescence spectrum of two-level systems driven by short pulses, *J. Phys. B* **19**, L657 (1986).
- [16] D. Rogus and M. Lewenstein, Resonant ionisation by smooth laser pulses, *J. Phys. B* **19**, 3051 (1986).
- [17] C. Meier and V. Engel, Interference Structure in the Photoelectron Spectra Obtained from Multiphoton Ionization of Na₂ with a Strong Femtosecond Laser Pulse, *Phys. Rev. Lett.* **73**, 3207 (1994).
- [18] M. Drescher, M. Hentschel, R. Kienberger, M. Uiberacker, V. Yakovlev, A. Scrinzi, Th. Westerwalbesloh, U. Kleineberg, U. Heinzmann, and F. Krausz, Time-resolved atomic inner-shell spectroscopy, *Nature (London)* **419**, 803 (2002).
- [19] M. Meyer *et al.*, Angle-Resolved Electron Spectroscopy of Laser-Assisted Auger Decay Induced by a Few-Femtosecond X-ray Pulse, *Phys. Rev. Lett.* **108**, 063007 (2012).
- [20] T. Mazza, K. G. Papamihail, P. Radcliffe, W. B. Li, T. J. Kelly, J. T. Costello, S. Düsterer, P. Lambropoulos, and M. Meyer, Controlling core hole relaxation dynamics via intense optical fields, *J. Phys. B* **45**, 141001 (2012).
- [21] A. Picón, C. Buth, G. Doumy, B. Krässig, L. Young, and S. H. Southworth, Optical control of resonant Auger processes, *Phys. Rev. A* **87**, 013432 (2013).
- [22] T. E. Glover, M. P. Hertlein, S. H. Southworth, T. K. Allison, J. van Tilborg, E. P. Kanter, B. Krässig, H. R. Varma, B. Rude, R. Santra, A. Belkacem, and L. Young, Controlling X-rays with light, *Nat. Phys.* **6**, 69 (2009).
- [23] C. Buth, R. Santra, and L. Young, Electromagnetically Induced Transparency for X Rays, *Phys. Rev. Lett.* **98**, 253001 (2007).
- [24] J. M. Schins, P. Breger, P. Agostini, R. C. Constantinescu, H. G. Muller, G. Grillon, A. Antonetti, and A. Mysyrowicz, Observation of Laser-Assisted Auger Decay in Argon, *Phys. Rev. Lett.* **73**, 2180 (1994).
- [25] O. Smirnova, V. S. Yakovlev, and A. Scrinzi, Quantum Coherence in the Time-Resolved Auger Measurement, *Phys. Rev. Lett.* **91**, 253001 (2003).
- [26] A. K. Kazansky and N. M. Kabachnik, Sideband structure in angle-resolved electron spectra from laser-assisted Auger decay generated by ultra-short pulses, *J. Phys. B* **42**, 121002 (2009).

- [27] A. K. Kazansky and N. M. Kabachnik, On the gross structure of sidebands in the spectra of laser-assisted Auger decay, *J. Phys. B* **43**, 035601 (2010).
- [28] C. Buth and K. J. Schafer, Theory of Auger decay by laser-dressed atoms, *Phys. Rev. A* **80**, 033410 (2009).
- [29] A. Picón, P. J. Ho, G. Doumy, and S. H. Southworth, Optically-dressed resonant Auger processes induced by high-intensity x-rays, *New J. Phys.* **15**, 083057 (2013).
- [30] S. B. Zhang and N. Rohringer, Quantum-beat Auger spectroscopy, *Phys. Rev. A* **92**, 043420 (2015).
- [31] S. Chatterjee and T. Nakajima, Ramsey interferometry for resonant Auger decay through core-excited states, *Phys. Rev. A* **94**, 023417 (2016).
- [32] V. F. Weisskopf and E. P. Wigner, *Z. Phys.* **63**, 54 (1930).
- [33] R. Santra and L. S. Cederbaum, Non-Hermitian electronic theory and applications to clusters, *Phys. Rep.* **368**, 1 (2002).
- [34] Ph. V. Demekhin and L. S. Cederbaum, Coherent intense resonant laser pulses lead to interference in the time domain seen in the spectrum of the emitted particles, *Phys. Rev. A* **86**, 063412 (2012).